

Mathematical models of magnetic insulation

Naoufel Ben Abdallah and Pierre Degond

MIP, Laboratoire CNRS (UMR 5640), Université Paul Sabatier, 118, route de Narbonne, 31062 Toulouse Cedex, France

Florian Méhats

Centre de Mathématiques Appliquées (URA CNRS 756), École polytechnique, 91128 Palaiseau Cedex, France

(Received 4 November 1997; accepted 1 December 1997)

The problem of magnetic insulation in a plane diode is discussed. Starting from the Child–Langmuir asymptotics of the stationary Vlasov–Maxwell system, various limit problems are exhibited and solved. Explicit formulas for the magnetic field at the cathode and for the electron sheath width are provided. The analysis allows one to recover and to complete the various known results related to magnetic insulation. In addition, an ensemble of intermediate models ranging from the quasilinear to the laminar model, and involving the formation of virtual cathodes, is exhibited. A stability analysis is then performed to determine which of these models are stable. The virtual cathode models are shown to be unstable under dissipation effects, and most of them are shown to be unstable under geometry effects (i.e., when replacing the planar geometry by the cylindrical one). The stability argument shows that in some situations, the laminar model is unstable while in other situations the quasilinear one is unstable. This gives some indication for the choice of the appropriate magnetic insulation model. © 1998 American Institute of Physics.

[S1070-664X(98)02605-6]

I. INTRODUCTION

We study the stationary self-consistent problem of magnetic insulation under space-charge limitation via the Child–Langmuir asymptotics of the Vlasov–Maxwell system. This approach was introduced by Langmuir and Compton¹ and recently developed by Degond and Raviart² to analyze the space-charge-limited operation of a vacuum diode. In a dimensionless form of the Vlasov–Poisson system, the ratio of the typical particle velocity at the cathode to that reached at the anode appears as a small parameter.² The associated perturbation analysis provides a mathematical framework to the results of Langmuir and Compton,¹ stating that the current flowing through the diode cannot exceed a certain value called the Child–Langmuir current. After this work, various extensions have been provided namely to the cylindrical and spherical diodes,³ to semiconductor devices (a review can be found in Ref. 4), and to bipolar diodes.⁵

In this paper, we propose an extension of this approach, based on the Child–Langmuir asymptotics to magnetized flows, in view of the earlier works about self-consistent models of magnetically insulated diodes by Ron *et al.*⁶ and Lovelace and Ott.⁷ The models of Ron *et al.* (or Lovelace and Ott) are rederived from our approach and their analysis completed. In addition to these models, a set of “parasitic” models is exhibited and its stability is studied under dissipation and geometry effects (Fig. 1).

II. SETTING OF THE PROBLEM

We consider a plane diode consisting of two perfectly conducting electrodes, a cathode ($X=0$) and an anode ($X=L$) supposed to be infinite planes, parallel to (Y,Z). The

electrons, with charge $-e$ and mass m , are emitted at the cathode and submitted to an applied electromagnetic field

$$\mathbf{E}_{\text{ext}} = E_{\text{ext}}\mathbf{X}, \quad \mathbf{B}_{\text{ext}} = B_{\text{ext}}\mathbf{Z},$$

such that $E_{\text{ext}} \leq 0$ and $B_{\text{ext}} \geq 0$. Such an electromagnetic field does not act on the P_z component of the particle momentum. Hence, we shall consider a situation where this component vanishes, leading to a confinement of electrons to the plane $Z=0$. The relationship between momentum and velocity is then given by the relativistic relations

$$\mathbf{V}(\mathbf{P}) = \frac{\mathbf{P}}{\gamma m}, \quad \gamma = \sqrt{1 + \frac{|\mathbf{P}|^2}{m^2 c^2}}, \quad (1)$$

$$\mathbf{V} = (V_X, V_Y), \quad \mathbf{P} = (P_X, P_Y), \quad |\mathbf{P}|^2 = P_X^2 + P_Y^2,$$

which can also be written

$$\mathbf{V}(\mathbf{P}) = \nabla_{\mathbf{P}} \mathcal{E}(\mathbf{P}), \quad (2)$$

where \mathcal{E} is the relativistic kinetic energy

$$\mathcal{E}(\mathbf{P}) = mc^2(\gamma - 1), \quad (3)$$

and c is the speed of light.

We shall, moreover, assume that the electron distribution function F does not depend on Y and that the flow is stationary and collisionless. The injection profile $G(P_X, P_Y)$ at the cathode is assumed to be given, whereas no electron is injected at the anode. The system is then described by the so called 1.5-dimensional Vlasov–Maxwell model

$$V_X \frac{\partial F}{\partial X} + e \left(\frac{d\Phi}{dX} - V_Y \frac{dA}{dX} \right) \frac{\partial F}{\partial P_X} + e V_X \frac{dA}{dX} \frac{\partial F}{\partial P_Y} = 0, \quad (4)$$

$$X \in (0, L), \quad (P_X, P_Y) \in \mathbb{R}^2,$$

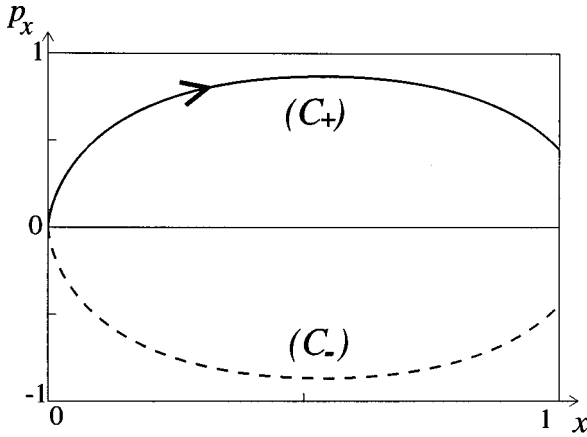


FIG. 1. Nonmagnetically insulated diode: phase portrait (x, p_x) under assumption (38).

$$\frac{d^2\Phi}{dX^2} = \frac{e}{\epsilon_0} N(X), \quad X \in (0, L), \tag{5}$$

$$\frac{d^2A}{dX^2} = -\mu_0 J_Y(X), \quad X \in (0, L), \tag{6}$$

subject to the following boundary conditions:

$$F(0, P_X, P_Y) = G(P_X, P_Y), \quad P_X > 0, \tag{7}$$

$$F(L, P_X, P_Y) = 0, \quad P_X < 0, \tag{8}$$

$$\Phi(0) = 0, \quad \Phi(L) = \Phi_L = -LE_{\text{ext}}, \tag{9}$$

$$A(0) = 0, \quad A(L) = A_L = LB_{\text{ext}}. \tag{10}$$

In this system, the macroscopic quantities, namely the particle density N , X and Y components of the current density J_X , J_Y , are, respectively, given by

$$N(X) = \int_{\mathbf{R}^2} F(X, P_X, P_Y) dP_X dP_Y, \tag{11}$$

$$J_X(X) = -e \int_{\mathbf{R}^2} V_X(\mathbf{P}) F(X, P_X, P_Y) dP_X dP_Y, \tag{12}$$

$$J_Y(X) = -e \int_{\mathbf{R}^2} V_Y(\mathbf{P}) F(X, P_X, P_Y) dP_X dP_Y. \tag{13}$$

In the above equations, ϵ_0 and μ_0 are, respectively, the vacuum permittivity and permeability. The boundary conditions are justified by the fact that the electric field $E = -d\Phi/dX$ and the magnetic field $B = dA/dX$ are exactly equal to the external fields when self-consistent effects are ignored ($N = J_Y = 0$). Besides, Eq. (6) is in fact the projection of Ampère’s law on the \mathbf{Y} axis. The projection on the \mathbf{X} axis gives

$$\frac{\partial B_Z}{\partial Y} - \frac{\partial B_Y}{\partial Z} = \mu_0 J_X.$$

Since the left-hand side of the above equation vanishes (because B depends only on X), J_X has to vanish, but this fact cannot be guaranteed *a priori*. The 1.5-dimensional model (4)–(10) ignores the self-consistent magnetic field due to J_X ,

which would introduce two-dimensional effects, and is only an approximation of the complete stationary Vlasov–Maxwell system. Nevertheless, our study of this model will give rise to two regimes. For a strong applied magnetic field, electrons do not reach the anode and come back to the cathode leading to a vanishing J_X component of current density; our model is fully rigorous in this case. When the applied magnetic field is not strong enough to insulate the diode, J_X does not vanish and our model can be viewed as an approximation of the Maxwell equations.

Similar to (11)–(13), we define the moments associated with the incoming particle distribution function by

$$N^G = \int_{\mathbf{R}_+^2} G(P_X, P_Y) dP_X dP_Y, \tag{14}$$

$$J_X^G = -e \int_{\mathbf{R}_+^2} V_X(\mathbf{P}) G(P_X, P_Y) dP_X dP_Y, \tag{15}$$

$$J_Y^G = -e \int_{\mathbf{R}_+^2} V_Y(\mathbf{P}) G(P_X, P_Y) dP_X dP_Y, \tag{16}$$

$$T^G = \int_{\mathbf{R}_+^2} \mathcal{E}(\mathbf{P}) G(P_X, P_Y) dP_X dP_Y, \tag{17}$$

where $\mathbf{R}_+^2 = \{(P_X, P_Y) \in \mathbf{R}^2, P_X > 0\}$ and the thermal emission velocity is $V^G = \sqrt{(T^G/mN^G)}$. The quantities (14)–(17), respectively, define the incoming particle density, the X and Y components of the incoming current density, and incoming particle kinetic energy.

In order to get a better insight in the behavior of the diode, we write the model in dimensionless variables in the spirit of Refs. 2 and 8. We first introduce the following units for position, velocity, momentum, electrostatic potential, vector potential, particle density, current, and distribution function, respectively:

$$\bar{X} = L, \quad \bar{V} = c, \quad \bar{P} = mc, \quad \bar{\mathcal{E}} = mc^2,$$

$$\bar{\Phi} = \frac{mc^2}{e}, \quad \bar{A} = \frac{mc}{e}, \quad \bar{N} = \frac{\epsilon_0 \bar{\Phi}}{X \bar{X}^2}, \quad \bar{J} = -ec \bar{N},$$

$$\bar{F} = \frac{\bar{N}}{\bar{P}^2},$$

and the corresponding dimensionless variables

$$x = X/\bar{X}, \quad \mathbf{p} = \mathbf{P}/\bar{P} = (p_x, p_y),$$

$$\mathbf{v} = (v_x, v_y) = \mathbf{V}/\bar{V} = \mathbf{p}/\sqrt{1 + \mathbf{p}^2}, \quad \epsilon = \mathcal{E}/\bar{\mathcal{E}} = \sqrt{1 + \mathbf{p}^2} - 1,$$

$$\varphi = \Phi/\bar{\Phi}, \quad a = A/\bar{A}, \quad n = N/\bar{N}, \quad \mathbf{j} = \mathbf{J}/\bar{J}, \quad f = F/\bar{F}.$$

The next step is to express that particle emission at the cathode occurs in the Child–Langmuir regime: In such a situation, the thermal velocity V_G is much smaller than the typical drift velocity supposed to be of the order of the speed of light c . Letting $\epsilon = V_G/c$, we shall assume that

$$f(0, p_x, p_y) = g^\epsilon(p_x, p_y) = \frac{1}{\epsilon^3} g\left(\frac{p_x}{\epsilon}, \frac{p_y}{\epsilon}\right), \quad p_x > 0,$$

where g is a given profile. The scaling factor ϵ^3 ensures that the incoming current remains finite independent of ϵ , whereas the dependence on p/ϵ expresses the fact that electrons are emitted at the cathode with a very small velocity. We refer to Refs. 2 and 8 for a detailed discussion of the scaling. The dimensionless system reads

$$v_x \frac{\partial f^\epsilon}{\partial x} + \left(\frac{d\varphi^\epsilon}{dx} - v_y \frac{da^\epsilon}{dx} \right) \frac{\partial f^\epsilon}{\partial p_x} + v_x \frac{da^\epsilon}{dx} \frac{\partial f^\epsilon}{\partial p_y} = 0, \tag{18}$$

$$(x, p_x, p_y) \in (0, 1) \times \mathbb{R}^2,$$

$$\frac{d^2 \varphi^\epsilon}{dx^2} = n^\epsilon(x), \quad x \in (0, 1), \tag{19}$$

$$\frac{d^2 a^\epsilon}{dx^2} = j_y^\epsilon(x), \quad x \in (0, 1), \tag{20}$$

$$n^\epsilon(x) = \int_{\mathbb{R}_+^2} f^\epsilon(x, p_x, p_y), \tag{21}$$

$$j_y^\epsilon(x) = \int_{\mathbb{R}_+^2} v_y f^\epsilon(x, p_x, p_y) dp_x dp_y, \tag{22}$$

$$= \int_{\mathbb{R}_+^2} \frac{p_y}{\sqrt{1 + |\mathbf{p}|^2}} f^\epsilon(x, p_x, p_y) dp_x dp_y,$$

$$f^\epsilon(0, p_x, p_y) = g^\epsilon(p_x, p_y) = \frac{1}{\epsilon^3} g\left(\frac{p_x}{\epsilon}, \frac{p_y}{\epsilon}\right), \quad p_x > 0, \tag{23}$$

$$f^\epsilon(1, p_x, p_y) = 0, \quad p_x < 0, \tag{24}$$

$$\varphi^\epsilon(0) = 0, \quad \varphi^\epsilon(1) = \varphi_L, \tag{25}$$

$$a^\epsilon(0) = 0, \quad a^\epsilon(1) = a_L. \tag{26}$$

We shall investigate the limit behavior of this system when $\epsilon \rightarrow 0$. The mathematical treatment is developed in Ref. 9 using the tools of Refs. 3 and 10. To derive the limit models, we first begin by writing the various invariants of the problem.

A. Invariants

The x component of the current and the total energy, respectively, given by

$$j_x^\epsilon(x) = \int_{\mathbb{R}} v_x f^\epsilon(x, p_x, p_y) dp_x dp_y, \tag{27}$$

$$= \int_{\mathbb{R}} \frac{p_x}{\sqrt{1 + |\mathbf{p}|^2}} f^\epsilon(x, p_x, p_y) dp_x dp_y,$$

and

$$k^\epsilon = \int_{\mathbb{R}^2} v_x p_x f^\epsilon(x, p_x, p_y) d\mathbf{p} - \frac{1}{2} \left[\left(\frac{d\varphi^\epsilon}{dx} \right)^2 - \left(\frac{da^\epsilon}{dx} \right)^2 \right], \tag{28}$$

are easily checked to be independent of the position x . Moreover, the following two quantities are constants of motion: the electron energy

$$\mathcal{H}^\epsilon(x, \mathbf{p}) = \epsilon(\mathbf{p}) - \varphi^\epsilon(x), \tag{29}$$

the canonical momentum

$$\mathcal{P}_y^\epsilon(x, \mathbf{p}) = p_y - a^\epsilon(x), \tag{30}$$

which means that on each electron trajectory (in the phase space), the above quantities are constant. Let us denote $f, n, a, j, \varphi, \dots$ the limit as ϵ tends to zero of $f^\epsilon, n^\epsilon, \dots$. Since, in the limit $\epsilon = 0$, electrons are injected with zero velocity, it is readily seen that the electron energy \mathcal{H} and canonical momentum \mathcal{P}_y simultaneously vanish. Consequently, the distribution function f is concentrated on the curve (\mathcal{C}) defined by

$$p_y(x) = a(x),$$

$$[p_x(x)]^2 = [1 + \varphi(x)]^2 - 1 - [a(x)]^2.$$

We notice that the following identities hold on (\mathcal{C}):

$$v_x(x) = \frac{p_x(x)}{\sqrt{1 + \mathbf{p}^2(x)}} = \frac{p_x(x)}{1 + \varphi(x)}, \tag{31}$$

$$v_y(x) = \frac{v_y(x)}{\sqrt{1 + \mathbf{p}^2(x)}} = \frac{a(x)}{1 + \varphi(x)}. \tag{32}$$

A consequence of the last identity is that $j_y = [a/(1 + \varphi)]n$, which means

$$(1 + \varphi)a'' = a\varphi''. \tag{33}$$

Let us now define the *effective potential* by

$$\theta(x) = [1 + \varphi(x)]^2 - 1 - [a(x)]^2. \tag{34}$$

Thanks to the second equation defining (\mathcal{C}), which can be written

$$[p_x(x)]^2 = \theta(x), \tag{35}$$

it is readily seen that electrons do not enter the diode unless the effective potential θ is non-negative in the vicinity of the cathode. Therefore, we always have $\theta'(0) \geq 0$. The limiting case $\theta'(0) = 0$ is the space-charge-limited or the Child–Langmuir regime. In view of (25) and (26) (which still hold in the limit $\epsilon \rightarrow 0$), this condition is equivalent to the standard Child–Langmuir condition

$$\frac{d\varphi}{dx}(0) = 0. \tag{36}$$

Besides, (35) implies that the characteristic curves are located in the zones where θ is non-negative. Let θ_L be the value of θ at the anode

$$\theta_L = (1 + \varphi_L)^2 - 1 - a_L^2. \tag{37}$$

If $\theta_L < 0$, electrons cannot reach the anode $x = 1$; they are reflected by the magnetic forces back to the cathode and the diode is said to be *magnetically insulated*. This enables us to define the Hull cutoff magnetic field, which is the relativistic version of the critical field introduced in Ref. 11 in the non-relativistic case:

$$a_L^H = \sqrt{\varphi_L^2 + 2\varphi_L}.$$

The diode is magnetically insulated if $a_L > a_L^H$, and is not insulated if $a_L < a_L^H$. In dimensional variables, the Hull cut-off magnetic field is given by

$$B^H = \frac{1}{Lc} \sqrt{\Phi_L^2 + \frac{2mc^2}{e} \Phi_L}.$$

The aim of this paper is to give a detailed analysis of both regimes. Let us begin by studying noninsulated diodes.

III. WEAK MAGNETIC FIELDS $B_{\text{ext}} < B^H$

In dimensionless variables, the applied effective potential $\theta_L = (1 + \varphi_L)^2 - 1 - a_L^2$ is positive.

A. Derivation of the model

The approach is similar to the purely electrostatic cases.^{2,3,10,5} Indeed, the effective potential takes a larger value at the anode than at the cathode, $\theta(1) - \theta(0) = \theta_L > 0$, which implies that electrons are globally accelerated inside the diode. A natural assumption is that

$$\forall x \in (0,1], \quad \theta(x) > 0. \tag{38}$$

This hypothesis, which shall be discussed in Sec. V and VI, is of primary importance for deriving the limit model. Indeed, it prevents the characteristic curve (\mathcal{E}) from meeting the axis $p_x = 0$ for $x > 0$. Consequently (\mathcal{E}) splits into two parts which only intersect at the point $(x=0, p_x=0, p_y=0)$ (see Fig. 1):

$$\begin{aligned} (\mathcal{E}_+) &= \{(x, p_x, p_y) \in (\mathcal{E}), p_x \geq 0\}, \\ (\mathcal{E}_-) &= \{(x, p_x, p_y) \in (\mathcal{E}), p_x \leq 0\}. \end{aligned}$$

Therefore, the current flows j_x^- and j_x^+ , respectively, carried by (\mathcal{E}_+) and (\mathcal{E}_-) do not depend on the position x . Since no electron is injected at the anode, j_x^- vanishes. Hence

$$j_x = j_x^+ = \int_{(\mathcal{E}_+)} v_x f(x, p_x, p_y) dp_x dp_y$$

and the distribution function is that of a monokinetic beam issued from the cathode $x=0$ with vanishing initial velocity

$$f(x, \mathbf{P}) = n(x) \delta(p_x - \sqrt{\theta(x)}) \delta[p_y - a(x)].$$

Therefore

$$n(x) = \frac{j_x}{v_x(x)} = j_x \frac{1 + \varphi(x)}{\sqrt{\theta(x)}},$$

$$j_y(x) = n(x) v_y(x) = j_x \frac{a(x)}{\sqrt{\theta(x)}}.$$

Inserting these expressions into Poisson's and Ampère's equations (19) and (20) gives

$$\frac{d^2 \varphi}{dx^2}(x) = j_x \frac{1 + \varphi(x)}{\sqrt{[1 + \varphi(x)]^2 - 1 - [a(x)]^2}}, \tag{39}$$

$$\frac{d^2 a}{dx^2}(x) = j_x \frac{a(x)}{\sqrt{[1 + \varphi(x)]^2 - 1 - [a(x)]^2}}, \tag{40}$$

$$\varphi(0) = 0, \quad \varphi(1) = \varphi_L, \tag{41}$$

$$\frac{d\varphi}{dx}(0) = 0, \tag{42}$$

$$a(0) = 0, \quad a(1) = a_L. \tag{43}$$

Let us recall that the unknowns are the electrostatic potential φ , the magnetic potential a , and the current j_x (which does not depend on x): for a given j_x , Eqs. (39) and (40), (41), and (43) determine φ and a while (42) is used to determine j_x . In the remainder, a solution of (39)–(43) will be denoted by \mathcal{S}^{ni} ; the superscript ni stands for “noninsulated” and more generally we shall use this superscript for a parameter corresponding to this model.

It is to be noticed that the whole construction of this model depends heavily on the assumption that the effective potential is positive. Actually, θ could vanish at some points in the diode, leading to closed trajectories and trapped particles. This point will be discussed in Sec. V.

Let us now proceed to the analytical resolution. The strategy relies on a shooting method with $\beta = a'(0)$ and j_x as shooting parameters: Given the values of β and j_x , solve (39) and (40) with the Cauchy conditions

$$\varphi(0) = 0, \quad a(0) = 0, \quad \varphi'(0) = 0, \quad a'(0) = \beta, \tag{44}$$

and then adjust the values in order to fulfill the conditions: $\varphi(1) = \varphi_L$ and $a(1) = a_L$.

B. Resolution of the Cauchy problem

In this part we solve the system (39), (40), and (44) with a given j_x, β . We shall follow—at least at the beginning—the computations of Ron *et al.*⁶ and Lovelace and Ott.⁷ However, in our calculations the computations are not restricted to the insulated diode case and the analytic resolution of the models is complete. We shall, in particular, give explicit expressions for the electron sheath width. Let us now turn to the resolution of (39), (40), and (44) and introduce, like in Refs. 6 or 7, the new unknowns ζ and γ by

$$\zeta(x) = \sqrt{\theta(x)} = \sqrt{(1 + \varphi)^2(x) - a^2(x) - 1}, \tag{45}$$

and

$$1 + \varphi(x) = \sqrt{\zeta^2(x) + 1} \cosh[\gamma(x)], \tag{46}$$

$$a(x) = \sqrt{\zeta^2(x) + 1} \sinh[\gamma(x)].$$

Written in terms of ζ and γ , the system completely decouples into

$$(\zeta')^2 = \frac{2j_x}{\zeta} \left(\zeta^2 - \frac{\beta^2}{2j_x} \zeta + 1 \right), \tag{47}$$

$$\gamma'(x) = \frac{\beta}{\zeta^2(x) + 1}. \tag{48}$$

The above equations are obtained by simple but lengthy algebraic manipulations, with the important intermediate results

$$(1 + \varphi)a' - \varphi'a = \beta, \tag{49}$$

$$2j_x \zeta - (\varphi')^2 + (a')^2 = \beta^2. \tag{50}$$

We first solve (47) by separation of variables. To this aim, we distinguish two cases, depending on the fact that the right-hand side of this equation (a second degree polynomial) can vanish or not. Here we shall only summarize the results and refer to Ref. 9 for a complete mathematical treatment. Let us set $\tilde{\beta} = \beta / \sqrt{j_x}$ and define the following functions:

$$\Lambda_a(\tilde{\beta}, \zeta) = \int_0^\zeta \frac{\tilde{\beta}\sqrt{\omega}}{\sqrt{2\left(\omega^2 - \frac{\tilde{\beta}^2}{2}\omega + 1\right)}(\omega^2 + 1)} d\omega, \quad (51)$$

$$\Pi_a(\tilde{\beta}, \zeta) = \int_0^\zeta \frac{\tilde{\beta}\sqrt{\omega}}{\sqrt{2\left(\omega^2 - \frac{\tilde{\beta}^2}{2}\omega + 1\right)}} d\omega. \quad (52)$$

These functions are defined for all $\zeta \geq 0$ when $\tilde{\beta} \leq 2$. If $\tilde{\beta} > 2$, they are defined only for $\zeta \in [0, \zeta_m]$, where

$$\zeta_m(\tilde{\beta}) = \frac{\tilde{\beta}^2 - \sqrt{\tilde{\beta}^4 - 16}}{4}. \quad (53)$$

Let us set in this case

$$\Lambda_m(\tilde{\beta}) = \Lambda_a[\tilde{\beta}, \zeta_m(\tilde{\beta})], \quad \Pi_m(\tilde{\beta}) = \Pi_a[\tilde{\beta}, \zeta_m(\tilde{\beta})], \quad (54)$$

$$\Lambda_b(\tilde{\beta}, \zeta) = 2\Lambda_m(\tilde{\beta}) - \Lambda_a(\tilde{\beta}, \zeta), \quad (55)$$

$$\Pi_b(\tilde{\beta}, \zeta) = 2\Pi_m(\tilde{\beta}) - \Pi_a(\tilde{\beta}, \zeta).$$

The solution of the Cauchy problem (39), (40), and (44) can be written implicitly by means of the above-defined functions.

If $\tilde{\beta} \leq 2$, then the solution $\zeta(x)$, $\gamma(x)$ is defined on $[0, +\infty]$ by

$$\beta x = \Pi_a[\tilde{\beta}, \zeta(x)], \quad \gamma(x) = \Lambda_a[\tilde{\beta}, \zeta(x)]. \quad (56)$$

If $\tilde{\beta} > 2$, then the solution $\zeta(x)$, $\gamma(x)$ is defined only on the interval $[0, 2x_m]$ where

$$x_m = \frac{\Pi_m(\tilde{\beta})}{\beta}; \quad (57)$$

and is implicitly given by

$$\begin{aligned} \text{for } 0 \leq x \leq x_m, \quad \beta x &= \Pi_a[\tilde{\beta}, \zeta(x)], \\ \gamma(x) &= \Lambda_a[\tilde{\beta}, \zeta(x)], \end{aligned} \quad (58)$$

$$\text{for } x_m \leq x \leq 2x_m \quad \beta x = \Pi_b[\tilde{\beta}, \zeta(x)],$$

$$\gamma(x) = \Lambda_b[\tilde{\beta}, \zeta(x)].$$

We notice that the function ζ is symmetric with respect to x_m , and reaches its maximum at this point. The value of this maximum is $\zeta(x_m) = \zeta_m(\tilde{\beta})$. Note also that the current j_x appears in (56) and (58) through the parameters $\tilde{\beta}$ and β , thanks to the equality $\beta = \sqrt{j_x} \tilde{\beta}$.

C. A shooting method with two parameters

We now consider the boundary conditions (41) and (43). If we denote

$$\zeta_L = \sqrt{\theta_L} = \sqrt{(1 + \varphi_L)^2 - 1 - a_L^2}, \quad \gamma_L = \operatorname{argsh}\left(\frac{a_L}{\sqrt{1 + \theta_L}}\right),$$

then the shooting method consists in determining all the parameters (j_x, β) , or equivalently $(\beta, \tilde{\beta})$ such that the functions given by (56) and (58) verify

$$\zeta(1) = \zeta_L, \quad \gamma(1) = \gamma_L. \quad (59)$$

Let us first determine $\tilde{\beta}$. We notice that ζ_L and γ_L have to satisfy one of the following relations:

$$\gamma_L = \Lambda_a(\tilde{\beta}, \zeta_L)$$

or

$$\gamma_L = \Lambda_b(\tilde{\beta}, \zeta_L). \quad (60)$$

Case 1: $\zeta_L \geq 1$. We claim that $\tilde{\beta} < 2$. Indeed, if this is not the case, we first deduce from (53) that the maximum value of ζ is $\zeta_m(\tilde{\beta}) < 1$. Therefore the value ζ_L cannot be reached by ζ .

Since Λ_b is defined only for $\tilde{\beta} > 2$, we have certainly

$$\gamma_L = \Lambda_a(\tilde{\beta}, \zeta_L).$$

This identity uniquely defines the parameter $\tilde{\beta}$ since it is readily seen that $\Lambda_a(\tilde{\beta}, \zeta_L)$ is an increasing function of its first argument $\tilde{\beta}$ and takes all positive values for $\tilde{\beta}$ ranging from 0 to 2.

Case 2: $\zeta_L \leq 1$. In this case, the function $\Lambda_a(\tilde{\beta}, \zeta_L)$ is defined only for $\tilde{\beta}$ smaller than the critical value

$$\tilde{\beta}_c = \sqrt{2\left(\zeta_L + \frac{1}{\zeta_L}\right)},$$

whereas for $\Lambda_b(\tilde{\beta}, \zeta_L)$ to be defined, $\tilde{\beta}$ has to fulfill the additional requirement $\tilde{\beta} > 2$. It is readily seen that, as $\tilde{\beta}$ ranges from zero to $\tilde{\beta}_c$, $\Lambda_a(\tilde{\beta}, \zeta_L)$ increases from 0 to $\gamma_c(\zeta_L)$, given by

$$\gamma_c(\zeta_L) = \Lambda_m\left[\sqrt{2\left(\zeta_L + \frac{1}{\zeta_L}\right)}\right].$$

On the other hand for $\tilde{\beta}$ increasing from 2 to $\tilde{\beta}_c$, $\Lambda_b(\tilde{\beta}, \zeta_L)$ decreases from infinity to $\gamma_c(\zeta_L)$. Thanks to this argument, $\tilde{\beta}$ can be computed by solving

$$\begin{aligned} \gamma_L &= \Lambda_a(\tilde{\beta}, \zeta_L) \quad \text{if } \gamma_L \leq \gamma_c(\zeta_L), \\ \gamma_L &= \Lambda_b(\tilde{\beta}, \zeta_L) \quad \text{if } \gamma_L \geq \gamma_c(\zeta_L). \end{aligned}$$

This resolution is illustrated in Fig. 2, where both cases are represented; the values chosen for the computations are $\zeta_L = 2$ and $\zeta_L = 0.3$.

Now that $\tilde{\beta}$ is determined, we turn to β . Evaluating (56) or (58) at $x = 1$, we have

$$\begin{aligned} \beta^{\text{ni}} &= \Pi_a(\tilde{\beta}, \zeta_L) \quad \text{in the case } \gamma_L = \Lambda_a(\tilde{\beta}, \zeta_L), \\ \beta^{\text{ni}} &= \Pi_b(\tilde{\beta}, \zeta_L) \quad \text{in the case } \gamma_L = \Lambda_b(\tilde{\beta}, \zeta_L). \end{aligned}$$

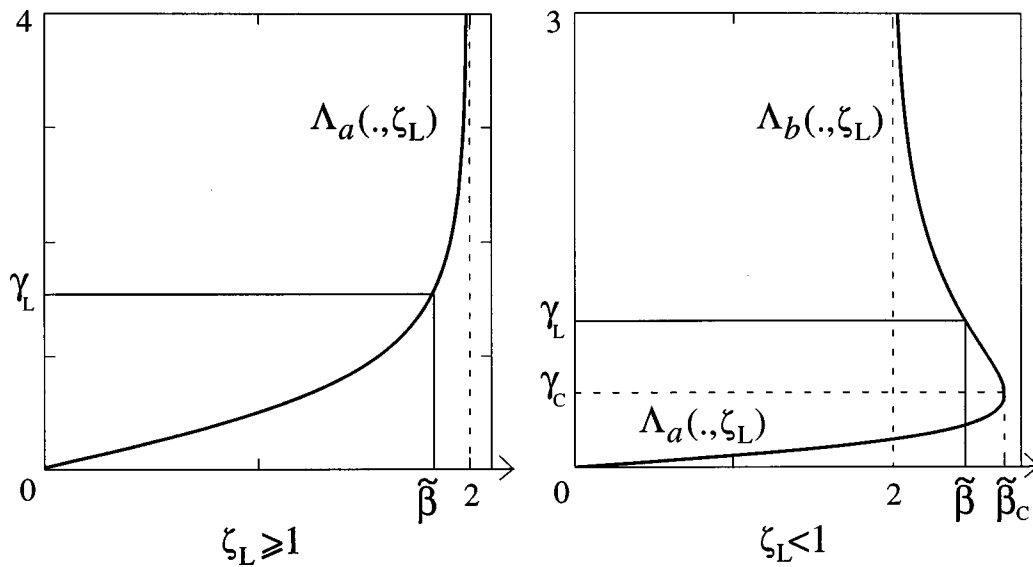


FIG. 2. Nonmagnetically insulated diode: determination of $\tilde{\beta}$ in function of the data (γ_L, ζ_L) . (a) case $\zeta_L \geq 1$; (b) case $\zeta_L < 1$.

Next, as written above, the current flowing through the diode is nothing but

$$j_x^{ni} = \left(\frac{\beta}{\tilde{\beta}} \right)^2.$$

IV. THE MAGNETICALLY INSULATED DIODE $B_{ext} > B^H$

Since $\theta_L < 0$, the effective potential applied to the diode is globally repulsive. Electrons emitted at the cathode with zero initial velocity cannot reach the anode. They are reflected back to the cathode at a point x^* of the diode such that

$$\forall x \in [0, x^*], \quad \theta(x) \geq 0, \quad \text{and} \quad n(x) > 0, \tag{61}$$

$$\forall x \in (x^*, 1], \quad \theta(x) < 0, \quad \text{and} \quad f(x, p_x, p_y) = 0.$$

We notice that in this case, the total current flow j_x from the cathode to the anode vanishes, which implies that our 1.5-dimensional model is consistent with the complete Maxwell system.

As previously noticed, the equations for the electrostatic and magnetic potentials heavily depend on the location of the points where the effective potential θ vanishes. The most general situation is studied in Ref. 9, and will be discussed in Secs. V and VI. Here we shall concentrate on two important particular cases: the *quasilaminar* model (see Ref. 6 or Ref. 7) where θ is assumed to vanish only at the electronic sheath edges and the *laminar* one (see Ref. 12), also referred to as *parapotential* or *Brillouin* flows in the literature, where the effective potential θ is assumed to vanish throughout the whole electronic sheath $[0, x^*]$.

In the quasilaminar case, electrons leave the cathode, reach the point x^* , then come back to the cathode, whereas in the laminar case they follow the equipotentials parallel to the \mathbf{Y} axis, and their velocity v_x along x is negligible.

Before separately studying both models, some quantities can be computed independently of any assumption on the zeros of θ inside the sheath. First, it can be proved (see Ref. 9) that

$$\theta'(x^*) = 0. \tag{62}$$

As in Sec. III, we set $\beta = a'(0)$ and use the variables ζ, γ defined by (45) and (46) on $[0, x^*]$. Denote by γ^*, a^*, \dots the values of the various functions at the edge x^* of the sheath. From (62) and (48), which are still valid on $[0, x^*]$, we have

$$1 + \varphi^* = \cosh \gamma^*, \quad a^* = \sinh \gamma^*,$$

$$\varphi'^* = \beta \sinh \gamma^*, \quad a'^* = \beta \cosh \gamma^*.$$

On the other hand, the potentials are affine functions outside the sheath. Hence

$$\varphi'^* = \frac{\varphi_L - \varphi^*}{1 - x^*}, \quad a'^* = \frac{a_L - a^*}{1 - x^*},$$

which implies

$$(1 - x^*)\beta \sinh \gamma^* = 1 + \varphi_L - \cosh \gamma^*, \tag{63}$$

$$(1 - x^*)\beta \cosh \gamma^* = a_L - \sinh \gamma^*.$$

Dividing the first equation by the second one yields after some rearrangements

$$(1 + \varphi_L)\cosh \gamma^* - a_L \sinh \gamma^* = 1. \tag{64}$$

This is a second degree equation in terms of $\exp(\gamma^*)$ which has at most two solutions. The requirement $0 \leq \varphi^* \leq \varphi_L$ allows one to select the unique solution

$$\gamma^* = \ln \frac{1 + \varphi_L + a_L}{1 + \sqrt{-\theta_L}}. \tag{65}$$

Inserting this formula in (63), we find after some algebraic manipulations

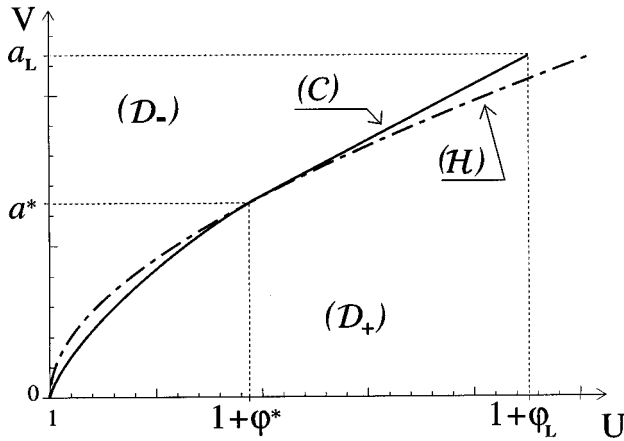


FIG. 3. Case of magnetic insulation: determination of $(1 + \varphi^*, a^*)$ in function of the data $(\Gamma + \varphi_L, a_L)$.

$$\beta(1-x^*) = \sqrt{-\theta_L}. \tag{66}$$

The construction of γ^* can also be done graphically (Fig. 3). In the plane $(U=1+\varphi, V=a)$, the point $(1+\varphi^*, a^*)$ lies on the positive quarter of hyperbola \mathcal{H} with equation $U^2 - V^2 = 1$. The condition $\theta'(x^*)=0$ expressed in the (U, V) plane means that at the point $(1+\varphi^*, a^*)$, the curve a vs $(1+\varphi)$ is tangent to the hyperbola \mathcal{H} . Moreover, since there is no electron outside the sheath, a is an affine function of $1+\varphi$ for φ larger than φ^* , which implies that $(1+\varphi^*, a^*)$ is the point of the hyperbola \mathcal{H} at which the tangent passes through $(1+\varphi_L, a_L)$.

A. The quasilinear model

The effective potential verifies θ is positive in the sheath $(0, x^*)$. We deduce from the phase space represented in Fig.

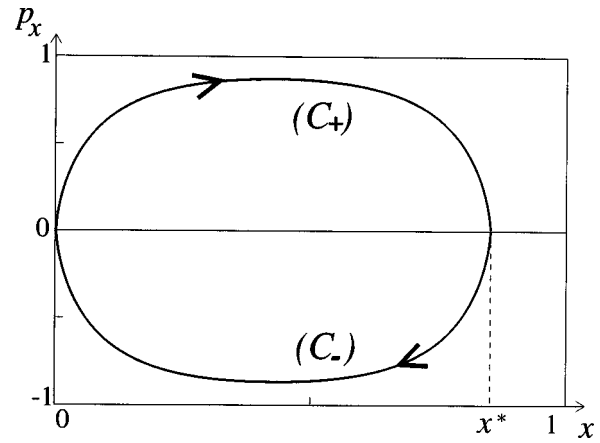


FIG. 4. Magnetically insulated diode: phase portrait (x, p_x) in the quasilinear model.

4, that the currents j_x^+ and j_x^- on the two branches of the characteristic curve (\mathcal{C}_+) and (\mathcal{C}_-) are constant and opposite. We shall denote $\bar{j} = 2j_x^+ = -2j_x^-$.

Consequently, the distribution function reads

$$f(x, p_x, p_y) = \frac{n(x)}{2} (\delta[p_x - \sqrt{\theta(x)}] \delta[p_y - a(x)])$$

and

$$n(x) = \frac{\bar{j}[1+\varphi(x)]}{\sqrt{\theta(x)}}, \quad j_y = \frac{\bar{j}a(x)}{\sqrt{\theta(x)}}.$$

Hence, the quasilinear model amounts to solving the following system for the unknowns φ, a, \bar{j} and x^* :

$$\forall x \in (0, x^*), \quad \frac{d^2\varphi}{dx^2}(x) = \bar{j} \frac{1+\varphi(x)}{\sqrt{[1+\varphi(x)]^2 - 1 - [a(x)]^2}}, \tag{67}$$

$$\frac{d^2a}{dx^2}(x) = \bar{j} \frac{a(x)}{\sqrt{[1+\varphi(x)]^2 - 1 - [a(x)]^2}}, \tag{68}$$

$$\forall x \in (x^*, 1), \quad \frac{d^2\varphi}{dx^2}(x) = \frac{d^2a}{dx^2}(x) = 0, \tag{69}$$

$$\varphi(0) = 0, \quad \varphi(1) = \varphi_L, \tag{70}$$

$$\frac{d\varphi}{dx}(0) = 0, \tag{71}$$

$$a(0) = 0, \quad a(1) = a_L \tag{72}$$

with the requirement that ψ, a , and their first derivatives are continuous at the sheath edge x^* .

Inside the sheath, the system (67) and (68), is exactly written like (39) and (40), with j_x replaced by \bar{j} . The results of Sec. III B can thus be adapted here. Let β and \bar{j} be given and set $\tilde{\beta} = \beta/\sqrt{\bar{j}}$. The solution of the Cauchy problem (67),

(68), and (44) associated with these data is known and given by (56) or (58).

To solve the complete quasilinear model, we now have to adjust the three shooting parameters β, \bar{j}, x^* . The first remark is that the effective potential θ vanishes at both edges of the sheath. Since a solution corresponding to $\tilde{\beta} > 2$ van-

ishes only at the origin, we deduce that $\tilde{\beta} < 2$ and that $[0, x^*]$ is the maximum interval of existence for θ : $x^* = 2x_m(\tilde{\beta})$ [see (57)]. To solve the quasilinear model completely, we only need to determine the parameters β , $\tilde{\beta}$, and x^* . To this aim, we first deduce from (48) and the symmetry of ζ with respect to $x_m = x^*/2$, that $\gamma^* = \gamma(2x_m) = 2\gamma(x_m)$. We now can compute $\tilde{\beta}$ by solving

$$\Lambda_m(\tilde{\beta}) = \frac{\gamma^*}{2},$$

where γ^* is given by (65) and Λ_m is defined by (54). To define β and x^* , we solve (66) together with

$$\frac{\beta x^*}{2} = \Pi_m(\tilde{\beta}),$$

where Π_m is defined in (54).

To summarize Sec. IV A, the solution \mathcal{S}_{QL}^i of the quasilinear case of magnetic insulation in the Child–Langmuir regime is determined by the following parameters:

$$\beta_{QL}^i = 2\Pi_m \circ \Lambda_m^{-1} \left(\frac{\gamma^*}{2} \right) + \sqrt{-\theta_L}, \tag{73}$$

$$x_{QL}^{*,i} = \frac{2\Pi_m \circ \Lambda_m^{-1} \left(\frac{\gamma^*}{2} \right)}{2\Pi_m \circ \Lambda_m^{-1} \left(\frac{\gamma^*}{2} \right) + \sqrt{-\theta_L}}, \tag{74}$$

$$\bar{j}_{QL}^i = \left(\frac{2\Pi_m \circ \Lambda_m^{-1} \left(\frac{\gamma^*}{2} \right) + \sqrt{-\theta_L}}{\Lambda_m^{-1} \left(\frac{\gamma^*}{2} \right)} \right)^2, \tag{75}$$

with γ^* given by (65) and θ_L by (37).

B. The laminar model

This model relies on the assumption that the effective potential θ vanishes on the sheath $[0, x^*]$ and is strictly negative outside the sheath. The current and charge densities vanish outside the sheath. Thanks to (35), the x component of the momentum vanishes on the curve \mathcal{C} , so the currents j_x^+ and j_x^- vanish everywhere in the diode. However the current $j_y(x)$ and the density of electrons $n(x)$ take nonzero values on $(0, x^*)$. Indeed, if n and j_y vanish identically, then with the Poisson and Ampère equations the potentials would be linear, which is not compatible with the assumption $\theta \equiv 0$ on $(0, x^*)$.

Consequently, the electrons only move on lines parallel to \mathbf{Y} . To compute the charge density in the sheath, the relation $j_x = n \cdot v_x$ is of no use since $j_x = v_x = 0$. We shall avoid this difficulty by using Eq. (33). The model is then written

$$\text{for } x \in [0, x^*], \quad \begin{aligned} [1 + \varphi(x)]^2 - [a(x)]^2 &= 1, & (76) \\ (1 + \varphi)a'' &= a\varphi'', & (33) \end{aligned}$$

$$\varphi''(x) = a''(x) = 0, \tag{77}$$

$$\text{for } x \in [x^*, 1], \quad \begin{aligned} \varphi(0) &= 0, \quad \varphi(1) = \varphi_L, \\ a(0) &= 0, \quad a(1) = a_L \end{aligned} \tag{78}$$

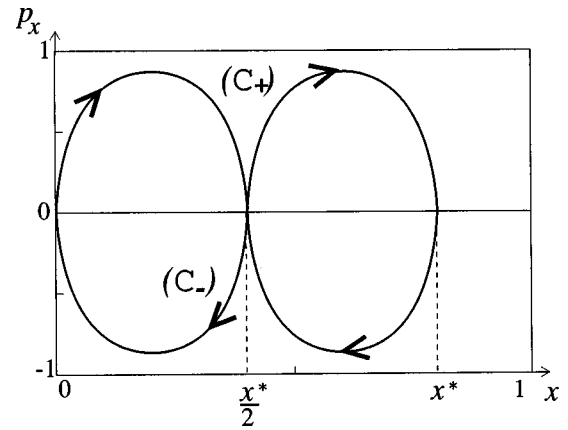


FIG. 5. Phase portrait for the parasitic model P1.

with the continuity requirement of a , φ , and their derivatives at the sheath edge x^* . This model is much simpler to solve than the previous ones. Indeed, we have by (76), $1 + \varphi(x) = \cosh[\gamma(x)]$ and $a(x) = \sinh[\gamma(x)]$ on $[0, x^*]$. Moreover, (48) leads to $\gamma(x) = \beta x$, thus $\gamma^* = \beta x^*$. From this relation and (65), (66), one deduces easily the values of the magnetic field β at the cathode and the width x^* of the sheath.

As a conclusion, the solution \mathcal{S}_L^i of the laminar model is given by

$$\beta_L^i = \gamma^* + \sqrt{-\theta_L}, \tag{79}$$

$$x_L^{*,i} = \frac{\gamma^*}{\gamma^* + \sqrt{-\theta_L}}, \tag{80}$$

with γ^* given by (65) and θ_L by (37). The density, current along y and distribution function of the electrons, for $x \in [0, x^*]$ are

$$n(x) = \beta^2 \cosh(\beta x), \quad j_y(x) = \beta^2 \sinh(\beta x),$$

$$f(x, p_x, p_y) = n(x) \delta(p_x) \delta[p_y - \sinh(\beta x)].$$

To our knowledge, formulas (79) and (80) for the magnetic field at the cathode and for the width of the sheath have never appeared in the literature on magnetic insulation.

V. PARASITIC SOLUTIONS

We have seen that the solutions \mathcal{S}^{ni} , \mathcal{S}_{QL}^i , and \mathcal{S}_L^i depend on some assumptions on the zeros of the effective potential $\theta = (1 + \varphi)^2 - a^2 - 1$ inside the electronic sheath. Unfortunately, in many cases,^{13,14} it is not clear whether these hypotheses are satisfied or not. When these hypotheses are not satisfied, a complete set of limit problems (which we call the parasitic models) is obtained. We refer to Ref. 9 where a detailed mathematical analysis of these problems can be found, and shall only summarize the results.

A. Nonmagnetically insulated diode

One cannot guarantee *a priori* that the effective potential θ does not vanish inside the diode. Actually, there may appear some virtual cathodes located at the points $x_k > 0$ where $\theta(x_k) = 0$. We show in Ref. 9 that the number of virtual

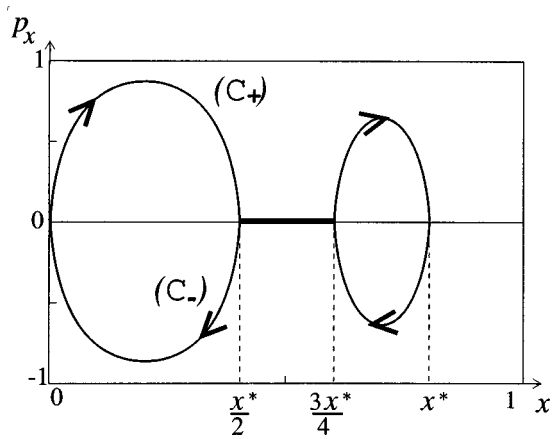


FIG. 6. Phase portrait for the parasitic model P2.

cathodes is finite and cannot exceed a certain value depending on the relative strength of the applied magnetic field. In particular, no virtual cathode can appear if

$$\left(1 + \frac{e\Phi_L}{mc^2}\right)^2 - \frac{e^2 A_L^2}{m^2 c^2} > 2.$$

Moreover, the number and the location of the virtual cathodes are not known *a priori*, but the solution can be constructed in a unique way once the location of the virtual cathodes is given. The formulas giving the solutions in this case and in the parasitic cases of magnetic insulation being somewhat lengthy, we skip them and refer to Ref. 9 (these formulas are, however, used for the numerical tests presented in the Sec. VI.

B. Magnetically insulated diode

So far, we have distinguished two cases. The quasilaminar case where the effective potential vanishes only at the sheath edges, and the laminar case where the effective potential vanishes on the whole sheath. Actually, all intermediate solutions may exist. We call them parasitic solutions. The main features of these solutions is that a finite or an infinite number of virtual cathodes can exist and the effective potential can even vanish on whole intervals inside the electronic sheath. We show in Ref. 9 that the distribution of zeros of the effective potential inside $[0, x^*]$ uniquely determines the length x^* of the sheath, and the solution (φ, a) . To illustrate this property we present two examples, represented in Figs. 5 and 6. In the first one, denoted P1, we only prescribe the fact that θ vanishes at the midpoint of the sheath. In the second one, θ only vanishes on the interval $[x^*/2, 3x^*/4]$. This information is sufficient to construct the solution (see Ref. 9) and in particular to determine the length x^* of the sheath.

VI. NUMERICS AND DISCUSSION

A. Numerical results

In this part, we represent the characteristic parameters of the previously defined models: \mathcal{S}^{mi} for weak magnetic fields, \mathcal{S}^{i}_{QL} , \mathcal{S}^i_L , \mathcal{S}^i_{P1} , and \mathcal{S}^i_{P2} for strong magnetic fields. No parasitic solutions has been represented here in the noninsulated case. In Figs. 7, 8, 9, 11, the applied electric potential is fixed and all the computed quantities are obtained by varying the dimensionless magnetic potential a_L . The electric potential chosen for the computations is $\varphi_L = 2$, or $\Phi_L = 2 mc^2/e$.

In Fig. 7, the dimensionless magnetic field β at the cathode has been represented. The dashed line is the applied

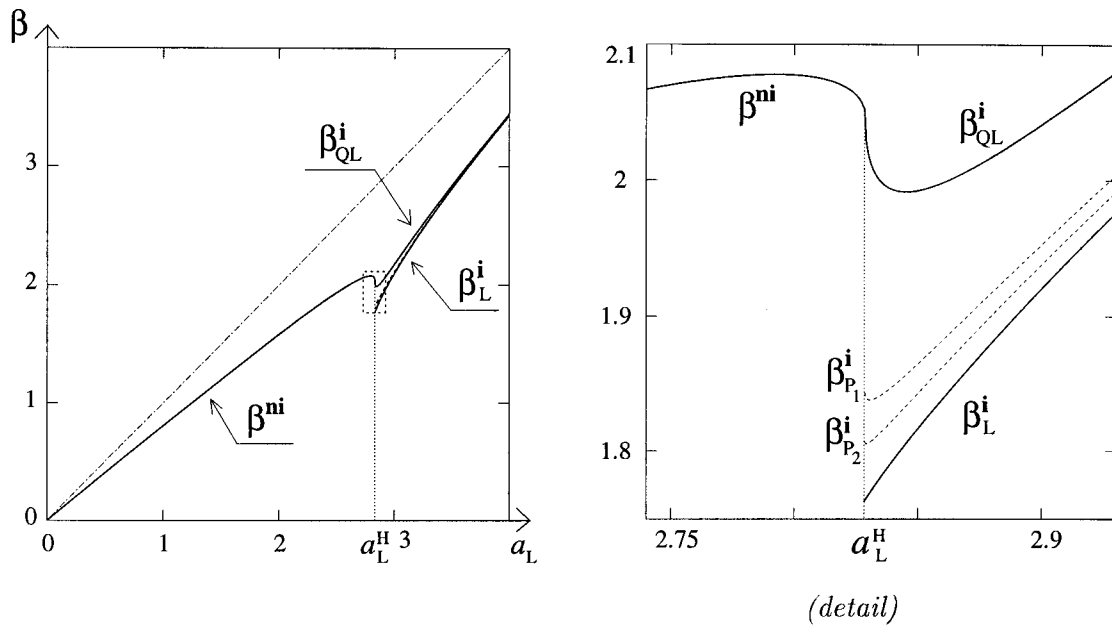


FIG. 7. (a) Magnetic field at the cathode in function of the applied magnetic field ($\varphi_L = 2$); (b) Details of (a).

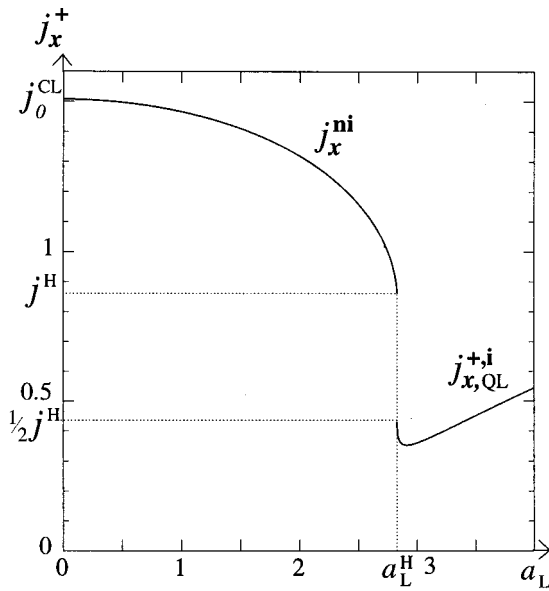


FIG. 8. Currents along x in function of the applied magnetic field ($\varphi_L = 2$).

magnetic field. Thus it appears on these curves, but also on the equations, that the magnetic field at the cathode is less than the applied magnetic field. Moreover, the detailed figure, zoomed in the neighborhood of the cutoff point a_L^H , shows that the curve $\beta_{QL}^i(a_L)$ is the only one that extends continuously $\beta^{ni}(a_L)$ at the point a_L^H . For $a_L > a_L^H$, and for both parasitic models, there holds

$$\beta_L^i < \beta_P^i < \beta_{QL}^i.$$

Hence, the relative uncertainty on the magnetic field at the cathode is bounded by $\text{Err}(\beta) = (\beta_{QL}^i - \beta_P^i) / \beta_L^i$. This uncertainty appears to be very small when $a_L \gg a_L^H$. Its maximal value $\max_{a_L > a_L^H} [\text{Err}(\beta)]$ has been represented as a function of the applied electric potential φ_L in Fig. 10 below.

Figure 8 shows the transmitted current j_x^{ni} in the noninsulated case $a_L < a_L^H$, and the current $j_{QL}^{+,i}$ of the electrons flowing with positive velocities, for $a_L > a_L^H$, and in the quasilinear model. Note that these curves have the same shape as the ones obtained for a cold and nonrelativistic model.¹⁵ When no magnetic field is applied, i.e., when $a_L = 0$, then j_x^{ni} is the relativistic electrostatic Child–Langmuir current j_0^{CL} . When a_L increases, the current decreases from j_0^{CL} to a certain value $j_x^{ni}(a_L^H) = j^H > 0$. Next, there is a gap as we pass to $a_L > a_L^H$ and $j_{QL}^{+,i} = 1/2 j^H$.

For strong magnetic fields, the length of the sheath x^* has been computed for models studied in Sec. IV and is represented in Fig. 9. Moreover, for both parasitic models, the corresponding $x_P^{*,i}$ is bounded by

$$x_L^{*,i} < x_P^{*,i} < x_{QL}^{*,i}.$$

The curves $x_L^{*,i}(a_L)$ and $x_{QL}^{*,i}(a_L)$ being very close to one another did not represent any parasitic model in Fig. 7. The relative uncertainty

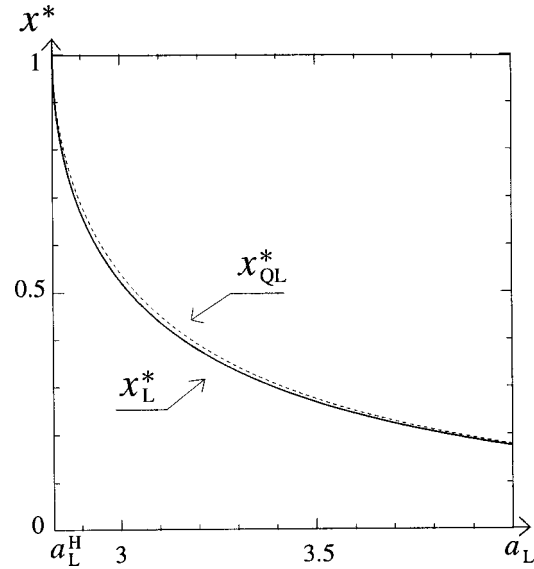


FIG. 9. Edge of the electron sheath x^* in function of the applied magnetic field ($\varphi_L = 2$).

$$\max_{a_L > a_L^H} \left(\frac{x_{QL}^{*,i} - x_L^{*,i}}{x_L^{*,i}} \right)$$

is plotted in Fig. 10 as a function of φ_L : this error appears to be very small.

Finally, we define an additional quantity of interest: the total drift current along the y coordinate, that can be computed thanks to (20):

$$I_y = \int_0^1 j_y(x) dx = a'(1) - a'(0) = \beta(\cosh \gamma^* - 1).$$

This quantity is plotted in Fig. 11, for the main three models. This current is maximal at the cutoff value $a_L = a_L^H$.

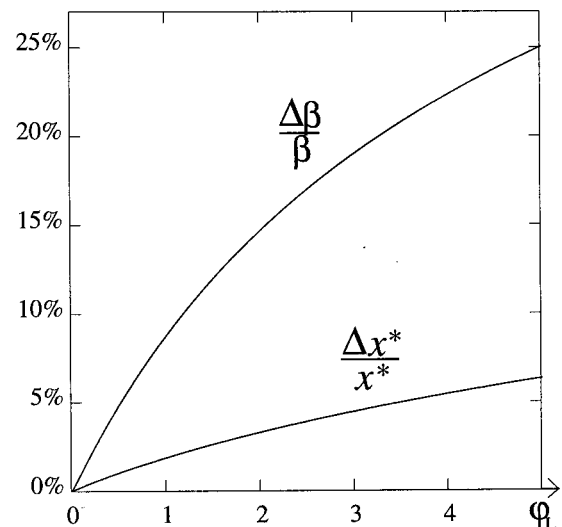


FIG. 10. Maximum relative uncertainty in x^* and β in function of the applied electric potential.

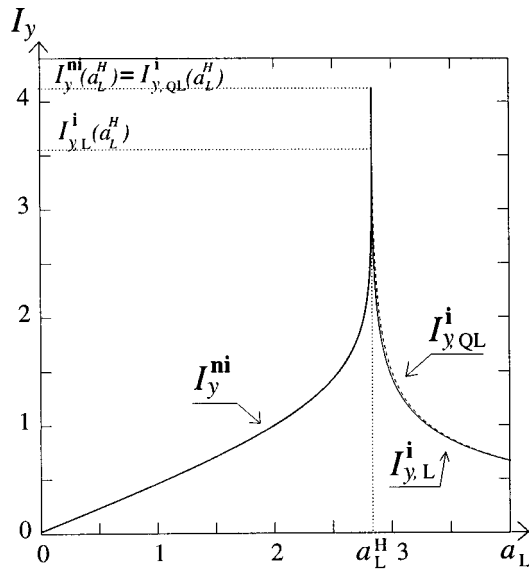


FIG. 11. Total drift-current along y in function of the applied magnetic field ($\varphi_L=2$).

B. Stability of parasitic solutions

We have seen that the most general limit model of (18)–(26) as $\epsilon \rightarrow 0$ admits an infinite multiplicity of solutions, and we numerically computed some of them. In the magnetically insulated case, these results show little variations of the values of x^* and of the magnetic field β , between the various models.

However, the multiplicity of models is not satisfactory and in the next paragraphs our aim is to give stability arguments that indicate in what sense some solutions are more physically acceptable than others. In Sec. VI B we study the influence of a small absorption term in the Vlasov equation. We then investigate geometrical effects. It is striking that the analysis eliminates a large number of parasitic solutions and sometimes all of them.

1. Presence of an absorption term

The previously considered models were obtained by passing to the limit $\epsilon \rightarrow 0$ in the Vlasov–Maxwell system. Let us introduce an absorption term in the Vlasov equation, i.e., we add a term λf with $\lambda > 0$ in the left-hand side of (18). Then pass to the limit $\epsilon \rightarrow 0$ and finally make the limit $\lambda \rightarrow 0$. We shall show that this operation eliminates all the parasitic solutions in the insulated and noninsulated cases. Moreover, the only stable solution in the insulated case is the quasilaminar solution.

Let us first show that if the effective potential θ vanishes at two points $x_0 < x_1$, then the derivative $\theta'(x_1)$ is negative.

We choose these points such that $\theta > 0$ on (x_0, x_1) . Notice that θ cannot vanish on a whole interval. Indeed, the j_x component of the current is no more constant but satisfies

$$\frac{dj_x}{dx}(x) = -\lambda n(x). \tag{81}$$

Since j_x vanishes at the points where θ vanishes, we deduce that if $\theta=0$ on an interval, the charge density n (and the j_y component) would also vanish. This is not possible since vacuum regions are characterized by $\theta < 0$.

Since θ is positive on (x_0, x_1) , then we can write

$$\frac{d^2\varphi}{dx^2}(x) = [j_x^+(x) - j_x^-(x)] \frac{1 + \varphi(x)}{\sqrt{\theta(x)}},$$

$$\frac{d^2a}{dx^2}(x) = [j_x^+(x) - j_x^-(x)],$$

where $j_x^+ > 0$ and $j_x^- < 0$ are the current fluxes of particles flowing, respectively, to the anode and to the cathode. These flows are no longer constant but satisfy the following differential equations:

$$\frac{dj_x^\pm}{dx} = \mp \lambda \frac{j_x^\pm(1 + \varphi)}{\sqrt{\theta}}.$$

Equation (47), expressed in terms of θ and modified in order to take into account the absorption term λ , turns into

$$\begin{aligned} & \left(\frac{d\theta}{dx}(x) \right)^2 - \left(\frac{d\theta}{dx}(x_0) \right)^2 \\ &= -4\beta^2\theta(x) + 8[1 + \theta(x)]\sqrt{\theta(x)}(j_x^+ - j_x^-)(x) \\ & \quad + 8\lambda[1 + \theta(x)] \int_{x_0}^x [1 + \varphi(y)]j_x(y)dy, \end{aligned}$$

where $j_x = j_x^+ + j_x^-$ is the total current. At $x = x_1$, we have

$$\left(\frac{d\theta}{dx}(x_1) \right)^2 - \left(\frac{d\theta}{dx}(x_0) \right)^2 = 8\lambda \int_{x_0}^{x_1} [1 + \varphi(y)]j_x(y)dy.$$

The integral on the right-hand side is strictly positive since j_x vanishes only in vacuum regions $\theta < 0$. Consequently, we have $|\theta'(x_1)| > 0$, which yields $\theta'(x_1) < 0$.

Let us now show that parasitic solutions do not exist in the noninsulated case: If they do, the effective potential would vanish at a point x_1 such that the derivative $\theta'(x_1)$ is negative. Hence θ takes negative values. The mathematical analysis shows that if the effective potential is negative at some point, it is negative on the whole interval between this point and the anode $x = 1$. This is clearly impossible since it violates the boundary condition $\theta_L > 0$.

Let us now turn to the magnetically insulated diode. For the same reason as mentioned above x_0 has to be equal to 0 and x_1 is nothing but the sheath edge x^* , which proves that the effective potential is positive in the sheath which corresponds to the quasilaminar solution.

From the existing literature on magnetic insulation, we could not get objective reasons to choose the quasilaminar model or the laminar one. Our stability analysis might give some insight into this topic since it shows that the laminar model is unstable under dissipation effects. Of course, one should be careful about this conclusion since the analysis is done in the stationary case. For instance, recent numerical simulations¹⁶ indicate that some nonstationary phenomena

such as turbulence should be taken into account. However, the extension to the time-dependent case seems out of reach for the moment.

2. Geometrical effects

Another factor that can reduce the multiplicity of steady solutions is the geometry of the diode.¹⁷ Consider a cylindrically symmetric diode, submitted to applied electric and magnetic fields. The complete study of the model will not be done here. Inspired by Ref. 3, we shall first write a singular perturbation problem, then derive formally the limit model as $\epsilon \rightarrow 0$. Our aim here is only to analyze the information on its solutions that we can get from a first integral argument like in Sec. VI B 1.

The diode consists of two coaxial electrodes. The cathode emits electrons and is either outside or inside the anode. The applied electric field is radial $\mathbf{E} = E(r)\mathbf{e}_r$ and the magnetic field is azimuthal $\mathbf{B} = B(r)\mathbf{e}_\theta$ [the cylindrical coordinates are (r, θ, z)]. The distribution function of the particles is $f(r, p_r, p_\theta, p_z)$, and the self-consistent fields can be written as gradients of the potentials $\varphi, \mathbf{a} = a\mathbf{e}_z$:

$$E(r) = -\frac{d\varphi(r)}{dr}, \quad B(r) = -\frac{da}{dr}.$$

The system is scaled following Ref. 3 and the dimensionless singular perturbation system corresponding to the Child–Langmuir asymptotics is written

$$v_r \frac{\partial f^\epsilon}{\partial r} + \left(\frac{v_\theta p_\theta}{r} + \frac{d\varphi^\epsilon}{dr} - v_z \frac{da^\epsilon}{dr} \right) \frac{\partial f^\epsilon}{\partial p_r} - \frac{v_\theta p_r}{r} \frac{\partial f^\epsilon}{\partial p_\theta} + v_r \frac{da^\epsilon}{dr} \frac{\partial f^\epsilon}{\partial p_z} = 0, \tag{82}$$

$$\frac{1}{r} \frac{d}{dr} \left(r \frac{d\varphi^\epsilon}{dr} \right) = n^\epsilon(r) = \int_{\mathbf{R}^3} f^\epsilon(r, p_r, p_\theta, p_z) d\mathbf{p}, \tag{83}$$

$$\frac{1}{r} \frac{d}{dr} \left(r \frac{da^\epsilon}{dr} \right) = j_z^\epsilon(r) = \int_{\mathbf{R}^3} v_z f^\epsilon(r, p_r, p_\theta, p_z) d\mathbf{p}, \tag{84}$$

$$f^\epsilon(1, \mathbf{p}) = g^\epsilon(\mathbf{p}) = \frac{1}{\epsilon^4} g\left(\frac{\mathbf{p}}{\epsilon}\right), \quad \text{sign}(\rho - 1)p_r > 0, \tag{85}$$

$$f^\epsilon(\rho, \mathbf{p}) = 0, \quad \text{sign}(\rho - 1)p_r < 0, \tag{86}$$

$$\varphi^\epsilon(1) = 0, \quad \varphi^\epsilon(\rho) = \varphi_\rho, \quad a^\epsilon(1) = 0, \quad a^\epsilon(\rho) = a_\rho, \tag{87}$$

where ρ is the diode aspect ratio, i.e., the ratio between the anode and the cathode radii.

The invariants along the characteristics can be deduced from (82) and take the same form as (29) and (30):

$$\mathcal{H} = \sqrt{1 + \mathbf{p}^2} - 1 - \varphi, \quad \mathcal{P}_\theta = rp_\theta, \quad \mathcal{P}_z = p_z - a.$$

They allow one to derive the formal limit model, as in Sec. II, by writing that these invariants vanish for the electrons originating from the cathode with zero initial velocity. This first leads to the introduction of an effective potential, similar to the function $\theta(x)$ in the case of the plane diode, and that we denote here $\omega(r) = [1 + \varphi(r)]^2 - [a(r)]^2 - 1$. As for the plane diode the value of this potential at the anode gives a cutoff condition, separating the problem into two

cases, the magnetically insulated diode and the noninsulated one. The critical dimensionless value is $\omega_\rho = (1 + \varphi_\rho)^2 - a_\rho^2 - 1 = 0$. Moreover, one can find *a priori* the same multiplicity of models, depending on the distribution of the zeros of $\omega(r)$ inside the sheath.

Consider now a region (r_0, r_1) , such that $\omega(r_0) = \omega(r_1) = 0$ and $\omega > 0$ on (r_0, r_1) . The quantities

$$i_r^+ = r \int_{p_r=0}^{p_r=+\infty} \int_{\mathbf{R}^2} v_r f dp_r dp_\theta dp_z,$$

$$i_r^- = r \int_{p_r=-\infty}^{p_r=0} \int_{\mathbf{R}^2} v_r f dp_r dp_\theta dp_z$$

remain constant on this interval and if we set $\bar{i} = i_r^+ - i_r^-$ then the limit model reads, on (r_0, r_1) ,

$$\frac{d}{dr} \left(r \frac{d\varphi}{dr} \right) = rn(r) = \bar{i} \frac{1 + \varphi(r)}{\sqrt{[1 + \varphi(r)]^2 - 1 - [a(r)]^2}}, \tag{88}$$

$$\frac{d}{dr} \left(r \frac{da}{dr} \right) = rj_z(r) = \bar{i} \frac{a(r)}{\sqrt{[1 + \varphi(r)]^2 - 1 - [a(r)]^2}}. \tag{89}$$

As in Ref. 3, set $x = \sigma \log(r)$, $x_0 = \sigma \log(r_0)$, $x_1 = \sigma \log(r_1)$, where $\sigma = \text{sign}(\rho - 1)$. Next, if we denote by $U(x) = 1 + \varphi(r)$, $W(x) = a(r)$, $\Omega(x) = \omega(r) = [U(x)]^2 - [W(x)]^2 - 1$, the system (88) and (89) can be rewritten

$$\frac{d^2 U}{dx^2}(x) = \bar{i} e^{\sigma x} \frac{U(x)}{\sqrt{\Omega(x)}}, \tag{90}$$

$$\frac{d^2 W}{dx^2}(x) = \bar{i} e^{\sigma x} \frac{W(x)}{\sqrt{\Omega(x)}}. \tag{91}$$

From these equations, a prime integral can be calculated and we obtain

$$\begin{aligned} & \left(\frac{d\Omega}{dx}(x) \right)^2 - \left(\frac{d\Omega}{dx}(x_0) \right)^2 \\ &= -4\beta^2 \Omega(x) + 8\bar{i}(1 + \Omega(x))\sqrt{\Omega(x)}e^{\sigma x} - 8\sigma\bar{i} \\ & \quad \times (1 + \Omega(x)) \int_{x_0}^x \sqrt{\Omega(y)}e^{\sigma y} dy. \end{aligned}$$

Besides, we have $(d\Omega/dx)(x_0) = 0$, since either $x_0 = 0$ and this equality is nothing but the Child–Langmuir condition, or $x_0 > 0$ and $(d\Omega/dx)(x_0) > 0$ would lead to the negativity of Ω for x smaller and close enough to x_0 . This leads to a contradiction since, if the effective potential is negative at some point, it stays negative from this point to the anode. We then have

$$\left(\frac{d\Omega}{dx}(x_1) \right)^2 = -8\sigma\bar{i} \int_{x_0}^{x_1} \sqrt{\Omega(y)}e^{\sigma y} dy. \tag{92}$$

Therefore, for the noninsulated diode, no parasitic model can be a solution of the limit model of (82)–(87). Indeed, in such a model, the effective potential Ω would be non-negative for $x \in [0, \log(\rho)]$, thus $(d\Omega/dx)(x_1) = 0$, which is incompatible with (92).

For the insulated diode two cases have to be considered. If the cathode is surrounded by the anode, then $\sigma = +1$ and (92) can never hold: The laminar model \mathcal{S}_L^i is the only possible stationary space-charge-limited model.

If the anode is inside the cathode ($\sigma = -1$), (92) implies

$$\frac{d\Omega}{dx}(x_1) < 0.$$

Thus, the point r_1 must be the edge of the sheath r^* . This fact also limits sizeably the multiplicity of possible limit models. Indeed, the only possible solutions are, the laminar model \mathcal{S}_L^i , the quasilaminar model \mathcal{S}_{QL}^i , and some parasitic models with the following structure: a laminar region $(1, r_0)$ where ω vanishes, then a quasilaminar region (r_0, r^*) where $\omega > 0$, then the insulated region (r^*, ρ) without electrons, where $\omega < 0$.

The approach that we adopted in this analysis follows closely the work by Swegle.¹⁷ However, our analysis departs from a more general situation. Indeed, in Ref. 17, the aim was to prove that a quasilaminar solution cannot exist, whereas we additionally prove that the whole set of parasitic solutions does not exist.

ACKNOWLEDGMENTS

The authors acknowledge support from the GdR SPARCH (Simulation du transport de PARTICULES CHargées) of the Centre National de la Recherche Scientifique, France.

¹I. Langmuir and K. T. Compton, Rev. Mod. Phys. **3**, 191 (1931).

²P. Degond and P.-A. Raviart, Asymptotic Anal. **4**, 187 (1991).

³P. Degond, S. Jaffard, F. Poupaud, and P.-A. Raviart, Math. Methods Appl. Sci. **19**, 287 (1996); **19**, 313 (1996).

⁴N. Ben Abdallah, P. Degond, and A. Yamnahakki, Solid-State Electron. **39**, 737 (1996).

⁵F. Méhats, "The Child-Langmuir asymptotics applied to the bipolar diode," to appear in Math. Meth. Appl. Sci.

⁶A. Ron, A. A. Mondelli, and N. Rostoker, IEEE Trans. Plasma Sci. **PS-1**, 85 (1973).

⁷R. V. Lovelace and E. Ott, Phys. Fluids **17**, 1263 (1974).

⁸P. Degond and P.-A. Raviart, Asymptotic Anal. **6**, 1 (1992).

⁹N. Ben Abdallah, P. Degond, and F. Méhats, "The Child-Langmuir asymptotics for magnetized flows."

¹⁰N. Ben Abdallah, Math. Methods Models Appl. Sci. **4**, 409 (1994).

¹¹A. W. Hull, Phys. Rev. **18**, 31 (1921).

¹²J. M. Creedon, J. Appl. Phys. **46**, 2946 (1975).

¹³M. Di Capua, IEEE Trans. Plasma Sci. **PS-11**, 205 (1983).

¹⁴J. M. Creedon, J. Appl. Phys. **48**, 1070 (1977).

¹⁵Y. Y. Lau, P. J. Christenson, and D. Chernin, Phys. Fluids B **5**, 4486 (1993).

¹⁶P. J. Christenson and Y. Y. Lau, Phys. Plasmas **1**, 3725 (1994).

¹⁷J. A. Swegle, Phys. Fluids **25**, 1282 (1982).